CONDUCTANCE TRANSIENTS ONTO DENDRITIC SPINES IN A SEGMENTAL CABLE MODEL OF HIPPOCAMPAL NEURONS

DENNIS A. TURNER
Institute of Neurophysiology, University of Oslo, Oslo 1, Norway

ABSTRACT Dendritic shaft (Z_d) and spine (Z_{sp}) input impedances were computed numerically for sites on hippocampal neurons, using a segmental format of cable calculations. The Z_{sp} values for a typical spine appended onto a dendritic shaft averaged <2% higher than the Z_d values for the adjacent dendritic shaft. Spine synaptic inputs were simulated by a brief conductance transient, which possessed a time integral of 12×10^{-10} S·ms. This input resulted in an average peak spine response of 20 mV for both dentate granule neurons and CA1 pyramidal cells. The average spine transient was attenuated <2% in conduction across the spine neck, considering peak voltage, waveform parameters, and charge transfer. The spine conductance transient resulted in an average somatic response of 100 μV in the dentate granule neurons, because of passive electrotonic propagation. The same input transient was also applied to proximal and distal sites on CA1 pyramidal cells. The predicted responses at the soma demonstrated a clear difference between the proximal and distal inputs, in terms of both peak voltage and waveform parameters. Thus, the main determinant of the passive propagation of transient electrical signals in these neurons appears to be dendritic branching rather than signal attenuation through the spine neck.

INTRODUCTION

Dendritic spines are the major postsynaptic structure for excitatory inputs in hippocampus (Cotman et al., 1973; Fifkova and Anderson, 1981; Miukwitz, 1976; Scheibel and Scheibel, 1968; Westrum and Balckstad, 1962). However, because of the physiological inaccessibility and small size of spines, direct evaluation of spine function has not been feasible. Several reports have suggested the concept of electrical attenuation across the small neck of a dendritic spine (Crick, 1982; Diamond et al., 1971; Fifkova and Anderson, 1981; Fifkova and Van Harreveld, 1977; Koch and Poggio, 1983; Purpura, 1974; Rall, 1974). The thinnest portion of a spine neck measures slightly greater than 0.10 μm in both CA1 pyramids (Lee et al., 1980; Westrum and Blackstad, 1962) and dentate granule neurons (Fifkova and Anderson, 1981; Fifkova and Van Harreveld, 1977). Because of this small size, the spine neck has been suggested to represent the largest core resistance in a neuron (Rall, 1974). If such is the case, the spine neck would be an important gating mechanism for synaptic inputs, because of large signal attenuation.

In a steady state evaluation of these hypotheses, Turner and Schwartzkroin (1983) found little or no signal attenuation across the spine neck, using typical electron microscopic (EM) dimensions for hippocampus. However, a more realistic method of simulating synapses involves a time-dependent conductance change, which causes a current flow proportional to the driving potential (the difference between the membrane potential and the equilibrium potential for that synapse) (Barrett and Crill, 1974; Koch and Poggio, 1983; Rinzel and Rall, 1974). The resulting voltage transient at the input site can be derived numerically (Norman, 1972). Several analytical methods can predict the propagation of transient potentials throughout a branched dendritic structure (Barrett and Crill, 1974; Horwitz, 1981; Jack and Redman, 1971; Norman, 1972; Redman, 1973; Rinzel and Rall, 1974). However, most of these methods require symmetry of branching, lumping of branching elements, or adherence to the equivalent cylinder assumption, which may not hold in these hippocampal neurons (Turner and Schwartzkroin, 1980, 1983). Thus, I have implemented the segmental format of cable calculations because the analysis included both an arbitrary branching pattern and dendritic spines (Turner, 1984).

An excitatory input signal onto a dendritic spine can be treated in two separate steps. The first step is the interaction of a transient conductance change and the spine input impedance, which results in a spine voltage transient. The second step is the propagation of a transient potential to the soma or recording site. The goal of this report is to describe the initiation and propagation of a dendritic spine potential in a segmental cable model. This study considers both the potency of mid-molecular layer synapses onto dentate granule cells and the relative efficacy of distal and proximal CA1 pyramidal neuron synapses. Certain features of these dendritic trees do follow, and other features do not

follow, the more general predictions of the equivalent cylinder models (Horwitz, 1981; Jack and Redman, 1971; Rinzel and Rall, 1974). As found with steady state analysis (Turner and Schwartzkroin, 1983), there is minimal signal attenuation of voltage transients across the spine neck in these two classes of hippocampal neurons. Preliminary reports of this work have been published as abstracts (Turner, 1982, 1983).

METHODS

Experimental Techniques

The experimental techniques have been presented in detail in the preceding report (Turner, 1984). The cells upon which these calculations have been based included CA1 pyramids ($n = 4$) and dentate granule neurons ($n = 4$).

Cable Calculations

Dendritic Input Impedances. Dendritic shaft (Z_d) and spine (Z_{sp}) input impedances were evaluated by the segmental cable method presented in the preceding report (Turner, 1984). The direct path of cable segments from the input site to the soma was first defined with an algorithm. This segment path (including side branches and their respective admittances) was next evaluated from the soma outward. The terminating admittance of the proximal dendritic trunk consisted of loading caused by the soma and other major dendrites. Voltage attenuation [$\tilde{V}(0, s)/\tilde{V}(l, s)$] and input admittance $\tilde{Y}(0, s)$ for each segment were defined, as functions of angular frequency [$q = (1 + s)^{1/2}$; $s = j\omega\tau$]:

$$\tilde{V}(0, s)/\tilde{V}(l, s) = \cosh(qX) + \tilde{Y}_t^*(l, s)\sinh(qX); \quad (1)$$

$$\tilde{Y}(0, s) = \frac{q}{r_i\lambda}\left[\frac{\sinh(qX) + \tilde{Y}_t^*(l, s)\cosh(qX)}{\cosh(qX) + \tilde{Y}_t^*(l, s)\sinh(qX)}\right]. \quad (2)$$

The distal end of each segment was defined as $x = 0$ and the proximal end (toward the soma) as $x = l$. The electrotonic distance for each segment, X, was defined as $X = l/\lambda$, where $\lambda = [(d R_m)/(4R_i)]^{1/2}$. d is the segment diameter, R_m is the specific membrane resistance, R_i is the specific internal resistivity, and $\tilde{Y}_t^*$ is the normalized terminating admittance, here assumed to be 0 (Turner, 1984).

The short spine neck was considered to be a cable segment, and the spine head was treated as a lumped admittance proportional to its surface area (as discussed in Turner, 1984). The same transient input was applied directly to either a dendritic shaft or a dendritic spine appended at that site. Comparison of these two inputs indicated the relative efficacy of shaft and spine inputs. The spine dimensions used in this analysis were the same for the CA1 pyramidal cells and the dentate granule neurons. These dimensions were corrected for EM shrinkage, which was ~40%. The spine neck diameter was assumed to be 0.17 μm, the spine neck length 0.67 μm, and the head surface area 1.12 μm^2. These dimensions follow EM reports of minimum neck dimensions in CA1 pyramidal cells (Lee et al., 1980; Westrum and Blackstad, 1962) and dentate granule neurons (Fifkova and Anderson, 1981; Fifkova and Van Harreveld, 1977). The spine dimensions were chosen to closely approximate EM reports of hippocampal spine measurements.

Conductance Transient Inputs. Excitatory synaptic inputs were simulated with a smooth conductance change, similar to that suggested by Rall (1967) and Rinzel and Rall (1974). The time course of the conductance change, $g(T)$, followed the normalized equation:

$$g(T) = g_p \propto T\exp(1 - \propto T), \quad (3)$$

where $g(T)$ is a function of normalized time T ($T = t/\tau$), a peak conductance change, g_p, and a coefficient, $\propto$. The peak time is reached at $T = 1/\propto$. The value of $\propto$ was chosen for this study to be 50, which is in the midrange of values described for motoneurons (12–100) (Barrett and Crill, 1974; Iansek and Redman, 1973; Jack et al., 1971; Rall, 1967). The transient in Eq. 3 has a time course identical to, but a magnitude different from, that employed by Jack et al. (1971).

The impulse response $Z(m\,\Delta T)$ was first derived for a particular dendritic site of electrotonic distance X, after a Fourier transform of the frequency-dependent impedance $\tilde{Z}_{sp}$ ($\tilde{Z}_{sp} = 1/\tilde{Y}_{sp}$). Second, the impulse response was convolved with the transient conductance change of Eq. 3:

$$V(X, k\Delta T) = \sum_{m=0}^{n-1} Z(m\Delta T)\, g[(k - m)\Delta T] \{V_{eq} - V(X, [(k - m) - 1]\Delta T\}\,\Delta T. \quad (4)$$

The resulting voltage response at this site, $V(X, k\Delta T)$ was a function of discrete increments of time, $k\Delta T$ (k in the range of 0 to $n - 1$). This equation specifically included the reduction of the driving potential caused by the fixed equilibrium potential (V_{eq}). The number of elements in the convolution, n, was chosen to be 4,096. This number of elements allowed the time increment to be sufficiently small ($\Delta T = 2.9 \times 10^{-4}\,\tau$) to include the fast decay of the dendritic responses and to decrease the integration error to <1%.

Voltage Transfer. The overall voltage transfer (VT_{sp}) from an input site to the soma was expressed as a function of frequency, applying Eq. 1 segment by segment and then inverting the overall product (voltage transfer is the inverse of attenuation). This frequency response was inverted to a function of normalized time using the reverse Fourier transform (Eq. 14 of Turner, 1984; also discussed by Norman, 1972). The transient potential at the dendritic site, $V(X, k\Delta T)$ (from Eq. 4) was convolved with the voltage transfer response, which resulted in the predicted voltage transient at the soma. Thus, these calculations followed a two-stage sequence. The first stage was the convolution of the excitatory conductance transient with the input impedance, $Z(m\Delta T)$. The second stage involved the propagation of the spine voltage potential from the dendritic site to the soma, using the voltage transfer response, VT_{sp}.

Synaptic Efficacy. The voltage peaks at the dendritic site and after transfer to the soma were compared, giving a ratio of transient voltage transfer. The input charge (Q_{in-c}) was calculated directly from the integral of the input current, considering the input signal to be a conductance change:

$$Q_{in-c} = \sum_{k=0}^{n-1}\sum_{m=0}^{n-1} g[(k - m)\,\Delta T]\,\{V_{eq} - V(X, [(k - m) - 1]\,\Delta T)\}\,\Delta T. \quad (5)$$

However, the charge injected was also calculated from the voltage integral (Q_{in-v}):

$$Q_{in-v} = \sum_{k=0}^{n-1} V(X, k\Delta T)\,\Delta T/Z_{sp}. \quad (6)$$

The main difference between the two numerical estimates of charge injection was the length of integration. The input conductance change ($\propto = 50$) decreased to essentially 0 by $T = 0.15\tau$. Thus, all of the charge injection (Eq. 5) was finished by that time. However, the voltage response to the conductance change, $V(X, k\Delta T)$, had a long tail out to several time constants. The somatic response to a dendritic input (Q_{soma-v}) was also

evaluated with Eq. 6. The period of integration of either the dendritic or somatic potential was adjusted to include >99% of the total charge by altering the time span of the convolution.

Waveform parameters of the somatic response to a dendritic input were also evaluated. These included the 10–90% rise time, the time to peak, and the halfwidth, all expressed in normalized time (Jack and Redman, 1971; Rall, 1967). Thus, as summarized by Rinzel and Rall (1974), there are several theoretical estimates of synaptic potency: the very low transient voltage transfer (~0.1%), the small steady state voltage transfer (~1%), and the greater charge transfer (~50%). The main considerations of this study were the peak voltage achieved at the soma and the charge transfer contributed to the soma, both in response to a dendritic input.

The transient conductance change (Eq. 3) was also directly applied to the soma in the segmental model. Since the somatic input admittance was so high, the nonlinearity caused by reduction of the driving potential in Eq. 4 was small, simulating a current input. The degree of nonlinearity for a dendritic input was derived by comparing the same transient input applied either to a dendritic site or to the soma. The integration for this comparison was performed on the summated charge factor, Q_{in-c}. This nonlinearity factor depended mainly on the spine input resistance. Thus, a larger voltage response at a dendritic site resulted in an increased amount of charge loss, because of the reduction of the driving potential (Rinzel and Rall, 1974).

The validity of the model was checked into two separate ways. The first involved the generation of an exponential decay. The second method derived transient potentials for an analytically defined equivalent cylinder neuron (Rinzel and Rall, 1974). The particular neuron tested possessed six identical dendrites and 366 segments with a terminating diameter of 0.20 μm. The terminating electrotonic distance was defined as 1.0λ. The small time and large time response functions of Rinzel and Rall (1974; Eqs. 21, 22, 24, and 25) were calculated and compared with the segmental model inputs, for similar sites. Both steady state and transient factors agreed within 1% for the two different numerical estimates of the same dendritic inputs.

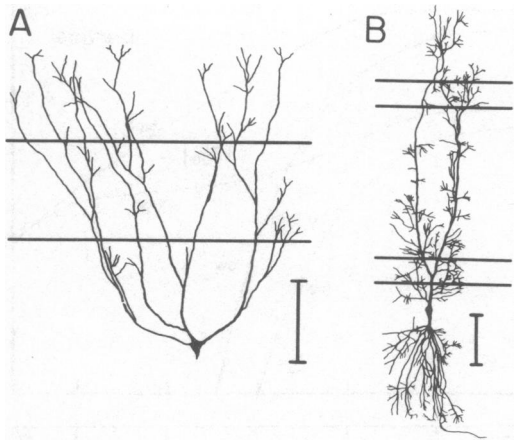

FIGURE 1 (*A*) Camera lucida drawing of a horseradish peroxidase (HRP)-stained dentate granule neuron from a previous study (Turner and Schwartzkroin, 1983). The scale represents 100 μm. The two horizontal bars demarcate the dendritic structure into proximal, middle, and distal thirds. Dendritic spine sites were selected at random from the middle third of the molecular layer (n = 72 total). These inputs sites were used in the analysis of the dentate quantal responses (see text). (*B*) A camera lucida tracing of a CA1 pyramidal neuron from a previous study (Turner and Schwartzkroin, 1980). The scale represents 100 μm. The two sets of horizontal bars portray 50-μm-wide proximal and distal regions of the dendritic tree. Spine input sites were selected from the proximal and distal regions (enclosed by the horizontal bars). The electrical parameters for these regions are presented in Table I.

RESULTS

Dendritic Input Impedances

Fig. 1 presents the geometric neuronal regions from which dendritic sites were selected. These regions were chosen to allow direct comparison to reported physiological studies. Fig. 1 *A* illustrates a dentate granule neuron after intracellular staining with horseradish peroxidase (Turner and Schwartzkroin, 1983). The horizontal lines demarcate the proximal, middle, and distal thirds of the dendritic tree. Dendritic sites (n = 72) were selected at random from the middle third of the dendritic trees of four such granule cells. These boundaries were selected to simulate "quantal" synaptic events evoked physiologically within a similar region (Crunelli et al., 1982; McNaughton, 1980; McNaughton et al., 1981).

The representative CA1 pyramidal cell shown in Fig. 1 *B* illustrates the two anatomical regions selected for simulation of excitatory synaptic inputs (EPSPs). The two sets of horizontal bars demarcate proximal and distal bands, each selected to be 50 μm wide. In four CA1 pyramids, 36 proximal and 36 distal sites were chosen. This selection of proximal and distal regions mimics physiological observations on CA1 pyramidal cells (Andersen et al., 1980). Thus, dendritic sites in these modeled hippocampal neurons were chosen to closely simulate physiological observations of EPSPs and to allow direct comparison of simulated results with experiment.

Input impedances for dendritic sites were calculated as described in Methods. Fig. 2 presents frequency-amplitude plots of the absolute value of input impedance ($|Z_{sp}|$) for representative spine sites. Fig. 2 *A* demonstrates a $|Z_{sp}|$ plot for a dentate granule neuron. The high and low $|Z_{sp}|$ plots in Fig. 2 *A* are both complex functions of frequency. Both $|Z_{sp}|$ functions, however, reached a steady decline of 20 dB/decade at a frequency of $\sim 2 \times 10^4$, which indicates relatively little high-frequency loss. These two sites possessed the same electrotonic distance (X) to the soma, X = 0.54λ, but were located on different-sized branches. The Z_{sp} values varied considerably among dendritic spines possessing the same X values because of large differences in the surrounding branching pattern. Separate values were calculated for a dendritic shaft site (Z_d) and for the impedance into a dendritic spine appended at that site (Z_{sp}). These two values differed approximately by the value of the spine stem impedance (Z_{ss}) (Rall, 1974). For the present spine dimensions (d = 0.17 μm and l = 0.67 μm), Z_{ss} was derived to be 22.1 MΩ, using the assumed value of 75 $\Omega \cdot$cm for the internal resistivity, R_i.

The Z_d and Z_{sp} values ranged from ~3 to 150 times the input impedance at the soma, Z_N, which is the reference against which the dendritic values should be compared (Jacobsen and Pollen, 1968; Rinzel and Rall, 1974). In a detailed theoretical model of a branched neuron, values for

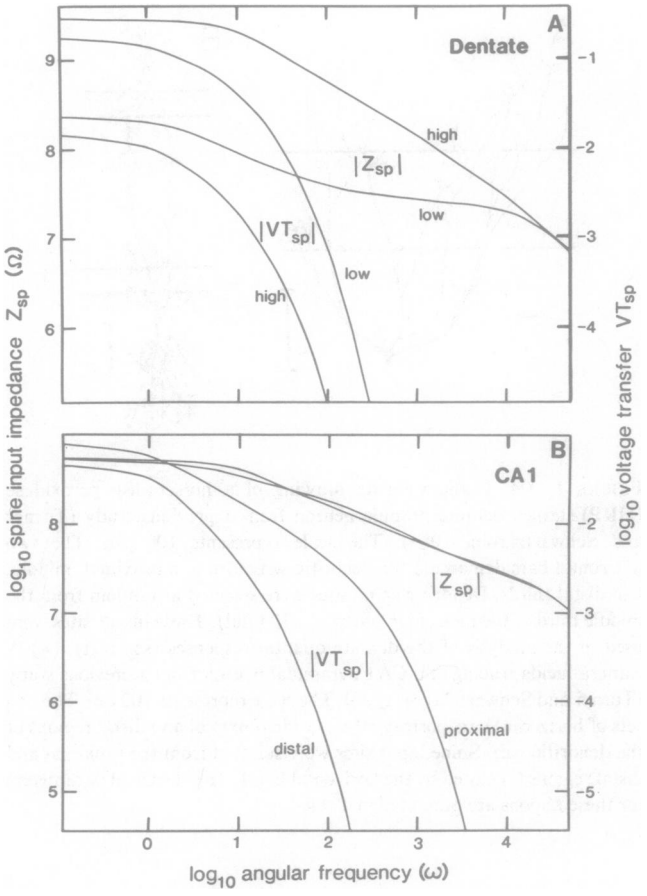

FIGURE 2 (*A*) Frequency-amplitude plot of the absolute value of spine input impedance, $|Z_{sp}|$. Two different dendritic sites are illustrated (high Z_{sp} and low Z_{sp}) for the dentate granule neuron of Fig. 1*A* (time constant of 12.6 ms). The two sites both possessed $X_{in} = 0.54\lambda$. However, the calculated Z_{sp} varied by a factor of 10 (the two slowly decaying curves). The faster-decaying curves are the absolute values of the voltage transfer, $|VT_{sp}|$, from the spine input site to the soma. The VT_{sp} curves represent more severe low-pass filters than the Z_{sp} responses. (*B*) Similar frequency-amplitude plot, but for two representative spine sites on the CA1 pyramidal neuron of Fig. 1*B* (time constant of 21.1 ms). Two sites were selected that possessed the same Z_{sp} value. However, one site was proximal ($X_{in} = 0.14$) and the other site was distal ($X_{in} = 0.67\lambda$). The curves of $|Z_{sp}|$ vs. frequency were almost identical for the two sites. The faster-decaying functions present $|VT_{sp}|$ from each site to the soma. The distal VT_{sp} curve demonstrated a more rapid decline in amplitude than the proximal, as a function of frequency. This was expected, because of the longer cable length between the distal site and the soma. This graph indicates that most of the high-frequency attenuation in the signal transfer between spine and soma occurs in the electrotonic or passive decay through the cable segments.

the ratio Z_d/Z_N ranged from 5 to 200 (Rinzel and Rall, 1974). Thus, the present values fall within this theoretical range. In absolute terms, the present Z_d values varied from 1.5×10^8 to 5.0×10^9 Ω. The Z_{sp} values were slightly higher when calculated directly and could be approximated by the equation $Z_{sp} = Z_d + Z_{ss}$. Even for the smallest value of Z_d, it is evident that the spine stem resistance added <15% to the input impedance at the spine head.

Table I presents the average values of Z_{sp} for the dendritic domains outlined in Fig. 1. The dentate midmolecular sites averaged $12.8 \pm 1.8 \times 10^8$ Ω (mean ± SEM), or 23.9 times the input impedance at the soma (Z_N). The CA1 proximal sites averaged $12.8 \pm 1.5 \times 10^8$ Ω, or 42.7 Z_N, while the distal sites averaged 58 times Z_N. The contribution of Z_{ss} to these average Z_{sp} values was <2%, since $Z_{ss} = 0.22 \times 10^8$ Ω. The most significant factor in determining Z_{sp} was therefore the Z_d value at the adjacent dendritic shaft. Hence, dendritic branching appeared to be the predominant factor in the calculation of the spine input impedances for these neurons (Koch and Poggio, 1983; Rall, 1974; Turner and Schwartzkroin, 1983).

Fig. 2 *B* illustrates the frequency response of representative distal and proximal spine sites on a CA1 pyramidal neuron (the cell shown in Fig. 1 *B*). These two sites possessed different X values ($X = 0.14\lambda$ for the proximal site and $X = 0.67\lambda$ for the distal site), but similar $|Z_{sp}|$ plots. Both curves are similar to the expected frequency response for a semi-infinite cable (Jack and Redman, 1971). There was not a simple correlation between the electrotonic distance to a site and the Z_{sp} value for that site, as suggested earlier by Rinzel and Rall (1974). The dendritic sites exhibited a higher frequency response than the input impedance at the soma (Fig. 5, Turner, 1984), which suggests a faster decay for the dendritic sites than for the somatic response.

Voltage Transfer to the Soma

Voltage transfer to the soma from either a dendritic shaft (VT_d) or a dendritic spine at the same site (VT_{sp}) were separately calculated. Fig. 2 *A* shows the high-frequency loss for $|VT_{sp}|$ (both high Z_{sp} and low Z_{sp} sites), mainly because of the inherent leakiness of the cable membrane. When contrasted with the frequency-amplitude plot of $|Z_{sp}|$ for any site, $|VT_{sp}|$ demonstrated a more substantial decrement at higher frequencies. The overall voltage transfer from a dendritic input site to the soma was nearly inversely proportional to the input impedance for that site (Rinzel and Rall, 1974). Thus, a site possessing a higher input impedance transferred relatively less voltage to the soma. The high Z_{sp} site in Fig. 2 *A* demonstrated an ~10 times lower VT_{sp} than the low Z_{sp} site.

Fig. 2 *B* illustrates an amplitude vs. frequency plot of voltage transfer to the soma for typical proximal and distal sites of a CA1 pyramidal neuron. These two sites calculated to possess similar Z_{sp} values (5.1×10^8 Ω) because of their location on similar-sized dendrites. However, the voltage transfer was remarkably different. The distal site ($X = 0.67\lambda$) displayed more voltage loss at higher frequencies than the proximal site ($X = 0.14\lambda$) because of the leakiness of a cable for higher frequencies. The degree of high-frequency loss was generally proportional to the electrotonic distance of the transfer path. Thus, the process of passive electrotonic decay acted as a substantial low-pass filter.

TABLE I
ELECTRICAL PARAMETERS FOR INPUTS ONTO DENDRITIC SPINES*

Cell type	X_{in}‡ (length constants)	Z_D§	Z_{sp}§	Dendritic spine peak	Soma waveform parameters‖				Charge parameters		
					Soma peak	10–90% Rise time	Time to peak	Halfwidth	Input¶ nonlinearity	Transfer to soma	Synaptic** effectiveness
		$10^8\ \Omega$	$10^8\ \Omega$	mV	μV	τ	τ	τ	%	%	%
Dentate mid-molecular layer	0.71	12.5	12.8	19.6	100.2	0.22	0.47	1.03	29.6	51.4	37.5
(n = 72)	0.03	1.7	1.8	1.6	10.2	0.01	0.03	0.03	2.4	1.7	2.0
CA1 proximal	0.32	12.6	12.8	21.3	82.1	0.10	0.21	0.59	30.4	81.8	57.1
(n = 36)	0.03	1.4	1.5	1.6	6.2	0.01	0.02	0.04	2.4	2.0	2.4
CA1 distal	1.00	17.2	17.4	23.2	16.1	0.40	0.82	1.45	33.5	33.8	22.5
(n = 36)	0.04	1.7	1.7	1.5	1.9	0.03	0.05	0.04	2.3	2.6	2.0
P-value‡‡ (t test)	0.001	0.04	0.04	NS	<0.001	<0.001	<0.001	<0.001	NS	<0.001	<0.001

*Values are mean ± SE of mean, with the standard error on the lower line.
‡X_{in} represents the average electrotonic distance to the dendritic spine sites, from the soma.
§Z_{sp} is the input impedance into the spine head and Z_D is the input impedence into the adjacent dendritic shaft.
‖These soma waveform parameters represent measurements of the soma response to a dendritic spine input.
¶The input nonlinearity is the decrease in charge injection compared to the same conductance transient applied directly to the soma.
**This is a ratio from Barrett & Crill (1974). Synaptic effectiveness compares the amount of charge transferred to the soma from a spine input with the charge injected for the same input directly to the soma.
‡‡This value indicates the level of significance at which the null hypothesis (that the means are equal) can be rejected, for the two sets of CA1 parameters.

Voltage transfer across the spine neck averaged >98% for the minimum spine dimensions used in the model. This finding for transient voltage transfer parallels previous steady state results (Turner and Schwartzkroin, 1983). Using Rall's (1974) framework for understanding Z_{ss} and its relation to Z_d, little voltage loss would be expected, since $Z_d \gg Z_{ss}$ (Table I). Critical spine dimensions needed to achieve even 10% attenuation across the spine neck were far out of the reported range and required a neck length of >3 μm for this diameter of spine neck. With larger neck dimensions, the critical length for <90% transfer across the spine neck would be even longer. Hence, the present minimum dimensions are the "worst case" example.

Conductance Transients

Fig. 3 *A* illustrates the input transient, $g(T)$, of Eq. 3 (g-soma, faster curve) applied directly to the soma of a dentate granule neuron. This conductance transient, plotted for $\alpha = 50$, had a peak at $T = 0.02\tau$ and was essentially 0 from 0.15τ onward. The slower curve in Fig. 3 *A* (V_{soma}) demonstrates the somatic voltage response to the conductance transient, with a peak of ~870 μV. The total integrated charge injected with this particular transient was 6.7×10^{-14} C, whereas the integrated conductance change was 12.0×10^{-10} S·ms.

The value for V_{eq}, the equilibrium potential of an excitatory synapse, was assumed to be 55 mV positive to the resting potential. This value has been derived from consideration of the reversal potential in CA1 pyramidal neurons (Hablitz and Langmoen, 1982) and from quantal studies on dentate granule cells (Crunelli et al., 1982;

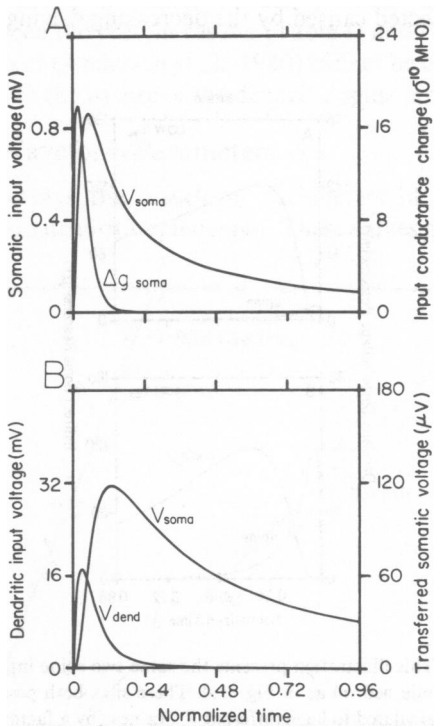

FIGURE 3 (*A*) The faster-rising and -decaying function (g_{soma}) portrays the conductance transient of Eq. 3, with $\alpha = 50$. The time integral of this transient was 12.0×10^{-10} S·ms. This transient input was directly applied to the soma of a dentate granule neuron. The slower-rising and -decaying transient is the somatic voltage response V_{soma} to the somatic input. All time values are expressed as normalized time ($T = t/\tau$). (*B*) An example of the conductance transient in *A* applied to a dendritic site. The resulting dendritic potential (V_{dend}) and somatic response (V_{soma}) are illustrated.

McNaughton et al., 1981). Because of the inaccessibility of dendritic spine synapses, this value for V_{eq} should be viewed as only an approximate figure, and it is less than the V_{eq} = 70 mV commonly used in motoneuron studies (Barrett and Crill, 1974).

Fig. 3 *B* shows a typical dendritic spine response (V_{dend}) to the conductance transient of Fig. 3 *A* and also the somatic response (V_{soma}) to the dendritic input. The electrotonic slowing in the passive cable propagation is also demonstrated by the shift in peak of the two transients.

Dentate Quantal Responses

Fig. 4 illustrates the neuronal response to the conductance transient of Fig. 3 *A*, when applied directly to dendritic spines. Fig. 4 *A* shows the voltage responses for the low Z_{sp} site analyzed in Fig. 2 *A*, and Fig. 4 *B* presents the responses for the high Z_{sp} site in Fig. 2 *A*. Both of these sites are from the mid-molecular region of the cell shown in Fig. 1 *A*. The faster transient (spine) in Fig. 4 *A* and *B* represents the voltage response of the dendritic spine to the conductance change transient. The total height of this response is approximately proportional to Z_{sp}. The site possessing the smaller input impedance (Fig. 4 *A*) peaked at only 3.5 mV. However, the same input at the site with the higher Z_{sp} (Fig. 4 *B*) resulted in a peak potential of 31.5 mV. The diminution in the peak voltage and the total charge injected caused by the decreasing driving potential has been termed the charge nonlinearity, after Barrett and Crill (1974). Both the average dendritic spine response and charge nonlinearity are presented in Table I. The degree of charge nonlinearity can be estimated by comparing a current transient of the same form as Eq. 3 with the conductance transient.

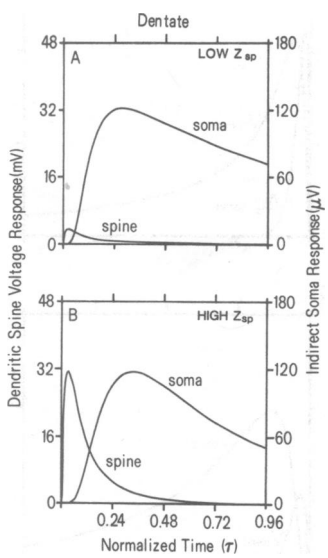

FIGURE 4 This illustration presents the same two spine input sites on a dentate granule neuron as in Fig. 2 *A*. These sites both possessed X_{in} = 0.54λ, but calculated to have different Z_{sp} values (by a factor of 10). (*A*) represents the low Z_{sp} site. The faster-rising and -decaying transient (spine) portrays the spine voltage response to the conductance transient (shown in Fig. 3), with a peak of 3.5 mV. The slower-rising and -decaying response (soma) is the resulting somatic voltage, with a peak of 131 μV. *B* illustrates the high Z_{sp} site. The dendritic spine voltage response was 31.5 mV. However, the voltage transfer from this site to the soma was less than in *A*, and resulted in a similar somatic waveform. Electrical parameters for these dentate spine inputs are given in Table I.

The slower transients (soma) in Fig. 4 *A* and *B*, portray the response at the soma resulting from passive propagation of the dendritic potential. The somatic transients for these two sites were almost identical, except for a slight difference in the time to peak. Thus, in spite of the large difference in size of the direct spine response (3.5 vs. 31.5 mV), the peak soma potential was approximately the same, ~120 μV. Fig. 4 also demonstrates the finding that voltage transfer was generally inversely proportional to the Z_{sp} values (Rinzel and Rall, 1974). These two sites possessed the same electrotonic distance to the soma, $X = 0.54\lambda$.

The conductance transient of Fig. 3 *A* was applied to 72 dendritic spine sites within the mid-molecular layer of the dentate granule neurons. The peak potential at the input spine averaged 19.6 ± 1.6 mV (Table I). The average charge injected was calculated to be 29.6 ± 2.4% less than when the same input transient was applied directly to the soma or applied as a current waveform (6.7×10^{-14} C). This loss of charge indicated significant nonlinearity caused by the decreased driving potential. The somatic peak voltage averaged 100.2 ± 10.2 μV, which is close to the value of 100 μV observed physiologically in dentate granule neurons (McNaughton et al., 1981). The somatic transient possessed a 10–90% rise time of 0.22 ± 0.01τ, a time to peak of 0.47 ± 0.03τ, and a halfwidth of 1.03 ± 0.03τ. These waveform parameters are similar to measurements from a study of in vitro dentate granule neurons (Barnes and McNaughton, 1980). The similarity to physiological reports suggests that the time course of the conductance transient (α = 50) lies in the approximately correct range.

The transient voltage transfer (from the spine to the soma) was calculated by comparing the peaks of the spine head and somatic potentials (Table I). On the average, this peak comparison resulted in a ratio of 0.5%. This figure can be compared with the steady state voltage transfer to the soma from the same sites, which was 1.8%. Table I also presents the charge parameters, as described in Methods. The charge transfer portrays the percentage of a steady state current input that is conveyed from these spine inputs to the soma (averaging 51%), which was calculated using Eq. 6. The estimate for overall synaptic effectiveness (Barrett and Crill, 1974) included the nonlinearity of the conductance transient and averaged less (37.5%). Thus, there are several estimates of the synaptic potency of quantal granule cell inputs to the mid-molecular region. The peak transient voltage may be the easiest to compare with experimental data, since the data from this model simulate physiological observations of peak somatic voltage (Crunelli et al., 1982; McNaughton et al., 1981).

CA1 Pyramidal Neuron Inputs

The input transient, g_{soma}, of Fig. 3 *A* was also applied to distal and proximal sites of CA1 pyramidal neurons, as defined in Fig. 1 *B*. The responses of the spines illustrated in Fig. 2 *B* (proximal and distal sites) are shown in Fig. 5. Fig. 5 *A* shows the potential at the distal site ($X = 0.67\lambda$), while Fig. 5 *B* portrays the response at the proximal site ($X = 0.14\lambda$). Since the Z_{sp} values for these two sites were approximately identical, the spine potentials (the faster transients in Fig. 5) were also similar, when the time to peak and the peak amplitude were compared. However, the slower transients of the somatic responses to the dendritic inputs appeared quite different. Fig. 5 *A* shows that the somatic response to the distal spine input resulted in a markedly attenuated and slowed transient, compared with the proximal response. This difference was a general finding for the comparison of the proximal and distal simulations. The slowing indicates the high degree of frequency loss of the transfer path along the cable segments (Rinzel and Rall, 1974). This leakiness for higher frequencies (as in Fig. 2 *B*) appears to be proportional to the electrotonic distance to a site.

The averages for a number of these spine inputs and for various waveform parameters for the proximal and distal sites are presented in Table I. Although there is a significant difference between the X values for the proximal and distal locations, the average peak spine potentials are approximately similar. This finding reinforces the concept that the input impedance is not a simple function of electrotonic distance (Rinzel and Rall, 1974), but also depends on branching parameters and dendritic diameters. The other parameters listed in Table I also are significantly different in the proximal and distal sites.

These modeling results are in contrast to a physiological report, in which selective stimulation of proximal and distal sites was performed (Anderson et al., 1980). In that study, little difference in waveform parameters for proximal and distal sites was found. Their absolute range of parameter values was close to the present estimates when corrected for an average time constant value of 15 ms (Turner, 1984). Thus, Andersen et al (1980) found mean values (for both proximal and distal sites) of $\sim 0.27\tau$ for the 10–90% rise time, 0.40τ for the time to peak, and 1.07τ for the halfwidth of the soma response. These are intermediate to the results of Table I, which may indicate that the physiological observations recruited larger regions of the dendritic tree than have been simulated by the model. However, the magnitudes of the somatic waveform parameters are close to those observed by Andersen et al. (1980), which suggests a reasonable correlation of this model with its physiological substrate.

The transient input onto a dendritic spine varied only slightly from the equivalent direct shaft input. This small difference appeared to be due to the minimally higher Z_{sp} value, as compared with Z_d (Table I). Thus, the discrepancy between the present results (Table I) and the physiological report (Andersen et al., 1980) cannot be completely attributed to the nature of the dendritic spine inputs.

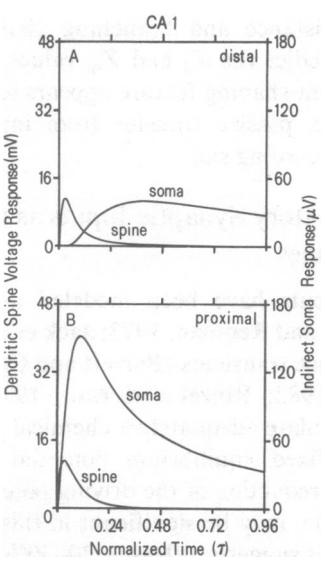

FIGURE 5 Spine inputs are presented for distal and proximal sites on the CA1 pyramidal neuron of Fig. 1*B*. These two sites both possessed the same Z_{sp} value. However, the somatic voltage responses to the spine inputs were markedly different. The site possessing the longer electrotonic distance (distal, *A*) demonstrated a much slowed and decreased response, compared with the proximal site shown in *B*. Such a distinct difference was consistently noted in these simulations of proximal and distal sites. Electrical parameters are presented in Table I.

Waveform Parameters

Fig. 6 portrays the waveform parameters of the soma response to a dendritic spine input. These values are plotted

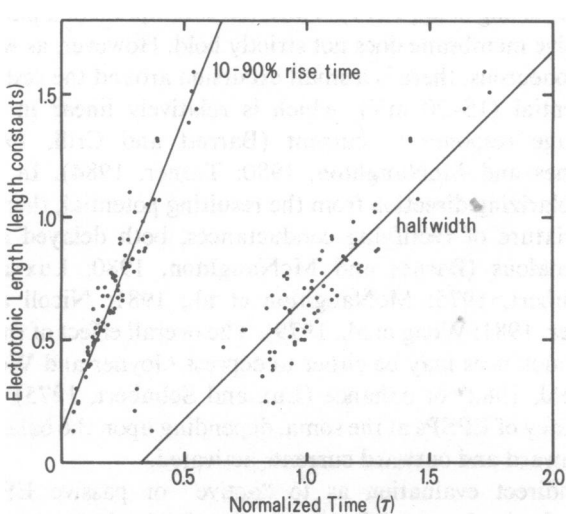

FIGURE 6 A plot of two EPSP waveform parameters of the soma response to a spine input, 10–90% rise time and halfwidth. These values are plotted versus electrotonic distance to the input site and are representative for both the dentate and CA1 neurons. There is a reasonable linear correlation for both parameters with respect to the electrotonic distance of the input site. These values were derived with $\alpha = 50$ in Eq. 1.

vs. the electrotonic distance to that site. There was little difference in these parameters between the dentate and CA1 neurons (for the present input waveform of $\alpha = 50$). The results have been pooled and are representative for both cell types. The regression lines indicate a close relationship between the X value and both the 10–90% rise time and the halfwidth. Such a close correspondence has been both predicted and observed in motoneuron EPSPs (Iansek and Redman, 1973; Jack and Redman, 1971; Rall, 1967). This linear relationship may allow the interpolation of an approximate X value for an EPSP site after evaluation of the waveform parameters of the EPSP (Jack et al., 1981). Generally, both the rise time and halfwidth values fell within the predicted shape-index borders for motoneurons (Jack et al., 1971) after correcting to normalized time.

DISCUSSION

Cable Model Assumptions

The assumptions and limitations inherent in this method of segmental cable analysis have been delineated in the preceding report (Turner, 1984). This cable model does appear to recreate adequately the physiologically observed response at the soma. The present calculations for simulated inputs at sites not directly accessible must be viewed within the framework of the cable model assumptions. These assumptions specifically include uniform membrane parameters, a passive membrane surface, smooth dendritic segments, and a Golgi-like distribution of small dendritic spines.

Several kinds of voltage-dependent conductances have been described for the somatic and dendritic membranes of these neurons (Nicoll and Alger, 1981; Traub and Llinas, 1979; Wong et al., 1979). Thus, the assumption of a purely passive membrane does not strictly hold. However, as with motoneurons, there is a small excursion around the resting potential (15–20 mV), which is relatively linear in the voltage response to current (Barrett and Crill, 1974; Barnes and McNaughton, 1980; Turner, 1984). In the depolarizing direction from the resulting potential, there is a mixture of rectifying conductances, both delayed and anomalous (Barnes and McNaughton, 1980; Lux and Schubert, 1975; McNaughton et al., 1981; Nicoll and Alger, 1981; Wong et al., 1979). The overall effect of these conductances may be either to depress (Joyner and Westerfield, 1982) or enhance (Lux and Schubert, 1975) the efficacy of EPSPs at the soma, depending upon the balance of inward and outward currents activated.

Indirect evaluation as to "active" or passive EPSP transfer is also possible (Jack et al., 1981). If we use the hypothesis of purely passive membrane and voltage transfer (as in this study), then predictions can be made regarding the passive shape and magnitude of EPSPs for inputs to certain locations. These predictions can be compared with physiological observations. If, as in motoneurons (Jack et al., 1981), the passive simulations can predict the physiological observations, then one need not invoke additional or complicating features. Major deviations from these assumptions might include either a nonuniformity of somatic and dendritic R_m or an active propagation of transient potentials throughout the dendritic tree (Andersen et al., 1980). These deviations of model predictions from the cable model assumptions may best be evaluated by careful comparisons with physiological data, as has been performed in motoneurons (Jack et al., 1981).

Dendritic Input Impedances and Voltage Transfer

The wide range of input impedances for both dendritic shaft and spine sites parallels the findings of a detailed neuron model (Rall, 1981; Rinzel and Rall, 1974). Most previous reports have considered only simpler analytical models for the study of dendrites (Horwitz, 1981; Jack and Redman, 1971; Rall, 1967). However, Barrett and Crill (1974) analyzed the arbitrary branching characteristics of Procion-stained motoneurons. They found that the input impedance values generally increased with electrotonic distance, as suggested by the simpler neuron models. The dendritic architecture of these hippocampal neurons suggests that the Z_d and Z_{sp} values are not simple functions of electrotonic distance. This finding is also true for the detailed branching model of Rinzel and Rall (1974), where there is a complex relationship between electrotonic distance, membrane parameters, branch size, and branch input impedance. Thus, in these "real" neurons, both electrotonic distance and branching characteristics are required to predict the Z_d and Z_{sp} values. Similarly, the major waveform-shaping feature appears to be the process of electrotonic, passive transfer from input site to the summing or recording site.

Excitatory Synaptic Inputs as Conductance Changes

Excitatory inputs have been modeled as both current inputs (Iansek and Redman, 1973; Jack et al., 1971, 1981) and conductance transients (Barrett and Crill, 1974; Koch and Poggio, 1983; Rinzel and Rall, 1974). The latter appears to simulate adequately a chemical junction potential since a fixed equilibrium potential is specifically included. The reduction of the driving potential, or loss of charge injection, may be significant in this situation. The present analysis suggests at least a 20–30% loss of injected charge for the conductance transients as compared with an equivalent current input. However, in no instance was there a "saturation" of the voltage response at the equilibrium potential (Koch and Poggio, 1983) for this range of parameter values. Jack et al. (1971) have used a range of values of the parameter α (Eq. 2), from 12 to 100 (Iansek

and Redman, 1973). The present value of $\alpha = 50$ was chosen as a representative midrange. However, the smaller unmyelinated and myelinated afferents in the hippocampus (Anderson et al., 1980) are likely to have much slower action potential time courses than the myelinated Ia afferents projecting onto motoneurons (Jack et al., 1981). A value of $\alpha = 10$ was also tried in a few calculations, but the predicted EPSP waveform parameters at the soma were much longer than those physiologically measured (Anderson et al., 1980; Barnes and McNaughton, 1980). Thus, a value of $\alpha = 50$ was felt to be the most consistent with the presently available physiological data in hippocampal neurons.

Dentate Quantal Responses

One major prediction of this study is the magnitude of the conductance change at a dendritic spine required to simulate a quantal response onto a dentate granule cell (Crunelli et al., 1982; McNaughton et al., 1981). The smooth input transient of Fig. 3 *A*, when applied to spines in the mid-molecular layer, resulted in the same average peak potential at the soma as that derived physiologically, a value of ~100 μV. This value inherently assumes, as discussed above, a purely passive transfer from the input spine to the soma. Additionally, one synapse per incoming afferent fiber is assumed. Although the latter value is unknown for these cells, the number of synaptic contacts of IA afferents onto motoneurons has been found to range from 5 to 20 histologically (Jack et al., 1981). Thus, the magnitude of the required conductance charge at each spine might be considerably less if, as in motoneurons, more than one synapse commonly constitutes a single afferent quantal response. A previous report was unable to distinguish between single and multiple afferent synapses, except to indicate the probable relative independence of multiple sites (McNaughton et al., 1981). Thus, closer studies are required for these dentate neurons, to determine the actual number of sites per afferent fiber and to ascertain the variability of each.

The amount of charge injection required for this quantal event, 6.7×10^{-14} C, is significantly less than that measured for motoneurons, $\sim 3 \times 10^{-12}$ C (Iansek and Redman, 1973). However, this injection must also charge up a longer time constant in these hippocampal neurons. Other aspects of this dentate quantal response are comparable to motoneuron values (Barrett and Crill, 1974), including a charge nonlinearity of 20–30% and the predicted dendritic response of 15–20 mV (Table I). The integral of the conductance change, 12.0×10^{-10} S·ms, appears significantly less than the magnitude predicted for motoneurons (40×10^{-10} S·ms; Barrett and Crill, 1974). Thus, in terms of specific parameters, the predicted quantal input value from this report appears to recreate the observed physiological responses adequately. The similarity of the passive predictions and reported waveform parameters also suggests that the propagation of transient potentials in dentate neurons may be a passive process.

CA1 Pyramidal Neuron Responses

The present calculations predict clear differences between proximal and distal simulations on CA1 pyramidal neurons, which conflict with preliminary physiological observations (Andersen et al., 1980). This physiological report indicates little difference between proximal and distal EPSPs following relatively focal stimulation of the dendritic trees of CA1 pyramidal neurons. There may be several reasons to account for this discrepancy. One major possibility lies in the single input nature of the present modeling calculations vs. the composite nature of the reported EPSP waveform indices. The use of composite excitatory events, especially with inhibitory events superimposed, may create difficulties in ascertaining exact waveform parameters of EPSPs (Alger and Micoll, 1982). However, the waveform parameters measured physiologically fall intermediate to the present results. This consistency suggests less discrete activation in the physiological study (Andersen et al., 1980) than has been simulated with the modeling data. Another reason for this discrepancy between predictions and measurement might involve an "active" process in the postsynaptic or dendritic region in the CA1 hippocampal neurons (Wong et al., 1979). If a similar process occurred at both proximal and distal sites, or at the junction of the two in the main apical shaft, a similarity of proximal and distal inputs might be observed (Andersen et al., 1980). Thus, there are several potential avenues of investigation regarding this difference between the model predictions and actual physiological observations.

As long as the value of α in Eq. 3 remained constant, there was a significant difference between the proximal and distal sites. However, the value of α may be different for the two regions. If α is faster for the distal and slower for the proximal sites, it might explain the similarity of EPSPs at the soma. Also, as has been suggested in motoneurons, there may be a variable sensitivity of the postsynaptic receptors to the chemical transmitter (Jack et al., 1981). In that report, the amount of charge transferred to the soma from both proximal and distal synapses was approximately identical. This is in contrast to theoretical neuron models (Rall, 1967) and also the present study, wherein less charge is transferred to the soma from distal as compared with proximal synaptic sites (Table I). Another possible reason for the discrepancy is the speed and nature of the incoming afferent fibers, which are relatively slow in conduction. More physiological study is required to confirm these proximal and distal results for smaller inputs, which may approach the quantal size used here. Such smaller inputs may be below the threshold for any active dendritic amplification.

Dendritic Spines

Because of their small size and inaccessibility, the role of dendritic spines has not been adequately clarified by physiologic studies. However, many hypotheses of spine function have pointed to the possibility of signal loss across the thin spine neck (Diamond et al., 1971; Fifkova and Anderson, 1981; Fifkova and Van Harreveld, 1977; Koch and Poggio, 1983; Rall, 1974). These hypotheses indicate that the thin spine neck is likely to produce a significant loss of the synaptic signal in its path from spine head to dentate shaft. As pointed out by Rall (1974), one of the critical determinations in assessing spine electrical attenuation is the comparison of the spine neck impedance (Z_{ss}) with the input impedance into the dendritic branch at the base of the spine (Z_d). Although Rall suggested a wide range of possible values for both Z_{ss} and Z_D, he presented no data on the actual range of either value for a particular cell. Thus, Rall (1974) and Rinzel and Rall (1974) have established a good theoretical framework for the electrical understanding of spines, but neither report has suggested any actual parameter values. Koch and Poggio (1983) do present calculated values for Z_d and compare these with a range of spine dimensions, but this report has serious flaws (see below).

The length constant of the dendritic spine was calculated to be ~0.005λ. Since charge transfer depends partially on electrotonic distance, little charge or current loss would be expected across the spine neck, which is in agreement with Koch and Poggio (1983). These average dimensions do not, however, include the wide variability of dendritic spine sizes (Jacobsen, 1967; Peters and Kaiserman-Abramof, 1970; Scheibel and Scheibel, 1968; Wenzel et al., 1973). I have used the minimum observed neck dimensions throughout the calculations in order to estimate the "worst case" situation. Thus, even the minimum spine dimensions do not suggest significant electrical loss when combined with the calculated dendritic input impedances (Rall, 1974; Turner and Schwartzkroin, 1983). Larger spine necks would exhibit even less voltage loss than the present minimum neck dimensions. However, longer spine necks might suggest a more significant role for spines, though the neck would need to be longer than 3.0 μm in order to incur even a 10% decrement in voltage transfer.

Another recent theoretical study has attempted to combine dendritic measurements with conductance change spine inputs (Koch and Poggio, 1983). However, there are considerable problems in interpreting their conclusion that for "reasonable" spine dimensions, transient spine inputs may "saturate" (to the equilibrium potential) or be significantly attenuated across the spine neck. The first difficulty is that the spine dimensions they used in the calculations were not appropriate for their single neocortical pyramidal cell. Unfortunately, Koch and Poggio applied the dimensions of either hippocampal spines or invertebrate spines (bee calycal interneurons) to their model, instead of using the larger neocrotical spine measurements reported by Jacobsen (1967). When combining the more appropriate spine measurements with the dendritic dimensions and impedances Koch and Poggio have reported, spine electrical loss of <10% would be expected, in concordance with the present study. Additionally, Koch and Poggio used only one neuron for all of their calculations, rather than averaging across several neurons, as in the present study. Also, their single neuron was taken from a Golgi study and had no physiological controls for R_N, τ, or R_m. It is difficult to infer even a wide range of accuracy for Koch and Poggio's calculations, since basic parameters were arbitrarily assumed and not matched to each cell. Thus, considering the lack of any controls on basic parameters, the use of only one Golgi-stained neuron, and the application of inappropriate spine dimensions, Koch and Poggio's specific conclusions do not appear warranted.

However, their framework of calculations is very reasonable and parallels that used in the present study. Hence, Koch and Poggio's general concepts regarding spine function may indeed be applicable in some setting other than CA1 and dentate hippocampal neurons. In these neurons, however, the present data clearly indicate that spines neither saturate with conductance charge inputs nor are they effective in controlling the attentuation of synaptic inputs. In addition, the present results are relatively insensitive to changes in spine neck diameter of length or in the magnitude of conductance charge input.

The meaning of the alterations in spine dimensions noted with electrical stimulation of the dentate gyrus (Fifkova and Anderson, 1981; Fifkova and Van Harreveld, 1977) is also unclear. These reports indicate that the spine necks increase in diameter after stimulation. This would imply only an increase in electrical transfer across the spine neck, from a large value of 98% to almost 100%. There may certainly be other significant factors regarding both possible structural and biochemical roles of dendritic spines (Crick, 1982; Gray, 1982; Purpura, 1974; Swindale, 1981) that are beyond this study.

In developmental studies of dentate neurons (Cotman et al., 1973), the appearance of spines clearly lags behind the formation of dendritic synapses. In early stages of postnatal development, the synapses are mainly of the asymmetric type and are attached to dendritic shafts directly. The formation of spines (Wenzel et al., 1981) comes much later, and extends into adulthood. It is not clear whether there is a further absolute increase in the number of synapses, or merely a development into the axo-spinous synapses of those already formed. Thus, the small dendritic spines appear to be structural enhancements of an often already present synapse. Peters and Kaiserman-Abramof (1970) have suggested that the formation of spines may promote the continued increase in complexity of the cortical neuropil during maturation, by preventing corkscrewing and other deviations by axons. Thus, spines may be structural elongation of the postsynaptic cell, in response to

some unknown influence by the presynaptic axon, rather than a specific element in the electrical processing of synaptic signals (Swindale, 1981).

I thank Per Andersen for this faithful support of this work. I also thank Drs. Wilfred Rall and Maurizio Mirolli for their critical review and discussion of this data.

This work was supported by National Institutes of Health Postdoctoral Fellowship (Individual) NS 06792, a Veterans Administration Research Service Award, and grant FSW-86-83 from the Minnesota Medical Foundation.

Received for publication 26 July 1983 and in final form 8 February 1984.

REFERENCES

Alger, B. E., and R. A. Nicoll. 1982. Feed-forward dendritic inhibition in rat hippocampal pyramidal cells studied in vitro. *J. Physiol. (Lond.).* 328:105–124.

Andersen, P., H. Silfvenius, F. H. Sundberg, O. Sveen. 1980. A comparison of distal and proximal dendritic synapses on CA1 pyramids in guinea-pig hippocampal slices in vitro. *J. Physiol. (Lond.).* 307:273–299.

Barnes, C. A., and B. L. McNaughton. 1980. Physiological compensation for loss of afferent synapses in rat hippocampal granule cells during senescence. *J. Physiol. (Lond.).* 309:473–485.

Barrett, J. N., and W. E. Crill. 1974. Influence of dendritic location and membrane properties on the effectiveness of synapses on cat motoneurons. *J. Physiol. (Lond.).* 239:325–345.

Cotman, C., D. Taylor, and G. Lynch. 1973. Ultrastructural changes in synapses in the dentate syrus of the rat during development. *Brain Res.* 63:205–213.

Crick, F. 1982. Do dendritic spines twitch? *Trends Neurosci.* 5:44–46.

Crunelli, V., S. Forda, G. L. Collingridge, and J. S. Kelly. 1982. Intracellular recorded synaptic antagonism in the rat dentate gyrus. *Nature (Lond.).* 300:450–452.

Diamond, J., E. G. Gray, and G. M. Yasargil. 1971. The function of the dendritic spine: an hypothesis. *In* Excitatory Synaptic Mechanisms. P Andersen and K. Jansen, editors. Universitetsforlaget, Oslo. 213–222.

Fifkova, E., and C. L. Anderson. 1981. Stimulation-induced changes in dimensions of stalks of dendritic spines in the dentate molecular layer. *Exp. Neurol.* 74:621–627.

Fifkova, E., and A. Van Harreveld. 1977. Long-lasting morphological changes in dendritic spines of dentate granule cells following stimulation of the entorhinal area. *J. Neurocytol.* 6:211–230.

Gray, E. G. 1982. Rehabilitating the dendritic spine. *Trends Neurosci.* 5:5–6.

Hablitz, J. J., and I. A. Langmoen. 1982. Excitation of hippocampal pyramidal cells by glutamate in the guinea-pig and rat. *J. Physiol. (Lond.).* 325:317–331.

Horwitz, B. 1981. An analytical method for investigating transient potentials in neurons with branching trees. *Biophys. J.* 36:155–192.

Iansek, R., and S. J. Redman. 1973. The amplitude, time course and charge of unitary excitatory postsynaptic potentials evoked in spinal motoneurones. *J. Physiol. (Lond.).* 234:665–688.

Jack, J. J. B., S., Miller, R. Porter, and S. J. Redman. 1971. The time course of minimal excitatory post-synaptic potentials evoked in spinal motoneurones by group IA afferent fibers. *J. Physiol. (Lond.).* 215:353–380.

Jack, J. J. B., and S. J. Redman. 1971. The propagation of transient potentials in some linear cable structures. *J. Physiol. (Lond.).* 215:283–320.

Jack, J. J. B., S. J. Redman, and K. Wong. 1981. The components of synaptic potentials evoked in cat spinal motoneurons by impulses in single group IA afferents. *J. Physiol. (Lond.).* 321:65–96.

Jacobsen, S. 1967. Dimensions of the dendritic spine in the sensorimotor cortex of the rat, cat, squirrel, monkey and man. *J. Comp. Neurol.* 129:49–58.

Jacobsen, S., and D. A. Pollen. 1968. Electrotonic spread of dendritic potentials in feline pyramidal cells. *Science (Wash. DC).* 161:1351–1353.

Joyner, R. W., and M. Westerfield. 1982. Effects of rectification on synaptic efficacy. *Biophys. J.* 38:39–46.

Koch, C., and T. Poggio. 1983. A theoretical analysis of electrical properties of spines. *Proc. R. Soc. Lond. B Biol. Sci.* 218:455–477.

Lee, K. S., F. Schottler, M. Oliver, and G. Lynch. 1980. Brief bursts of high-frequency stimulation produce two types of structural change in rat hippocampus. *J. Neurophysiol. (Bethesda).* 44:247–258.

Lux, H. D., and P. S. Schubert. 1975. Some aspects of the electroanatomy of dendrites. *Adv. Neurol.* 12:29–44.

McNaughton, B. L. 1980. Evidence for two physiologically distinct perforant pathways to the fascia dentata. *Brain Res.* 199:1–19.

McNaughton, B. L., C. A. Barnes, and P. Andersen. 1981. Synaptic efficacy and EPSP summation in granule cells of rat fascia dentata studied in vitro. *J. Neurophysiol. (Bethesda).* 46:952–966.

Minkwitz, H.-G. 1976. Zur Entwicklung der Neuronenstruktur des Hippocampus während der prä- und postnatalen Ontogenese der Albinoratte. III. Mitteilung: Morphometrische Erfassung der ontogenetischen Veranderungen in Dendritenstruktur und Spine besatz an Pyramiden-Neuronen (CA1) des Hippocampus. *J. Hirnforsch.* 17:255–275.

Nicoll, P. A., and B. E. Alger. 1981. Synaptic excitation may activate a calcium-dependent potassium conductance in hippocampal pyramidal cells. *Science (Wash. DC).* 212:957–959.

Norman, R. S. 1972. Cable theory for finite length dendritic cylinders with initial and boundary conditions. *Biophys. J.* 12:25–45.

Peters, A., and I. R. Kaiserman-Abramof. 1970. The small pyramidal neuron of the rat cerebral cortex. The perikaryon, dendrites and spines. *Am. J. Anat.* 127:321–356.

Purpura, D. P. 1974. Dendritic spine dysgenesis and mental retardation. *Science (Wash. DC).* 186:1126–1128.

Rall, W. 1967. Distinguishing theoretical synaptic potentials computed for different soma-dendritic distributions of synaptic input. *J. Neurophysiol. (Bethesda).* 30:1138–1168.

Rall, W. 1974. Dendritic spines, synaptic potency and neuronal plasticity. *In* Cellular Mechanisms Subserving Changes in Neuronal Activity. C. D. Woody, K. A. Brown, T. J. Crown, and J. D. Knispel, editors. Brain Information Service, Los Angeles. 13–21.

Rall, W. 1981. Functional aspects of neuronal geometry. *In* Neurons without Impulses. A. Roberts and B. M. H. Bush, editors. Cambridge University Press, Cambridge. 223–254.

Redman, S. J. 1973. The attenuation of passively propagating dendritic potentials in a motoneurone cable model. *J. Physiol. (Lond.).* 234:637–664.

Rinzel, J., and W. Rall. 1974. Transient response in a dendritic neuron model for current injected at one branch. *Biophys. J.* 14:759–790.

Scheibel, M. E., and A. B. Scheibel. 1968. On the nature of dendritic spines—report of a workshop. *Commun. Behav. Biol. Part A Orig. Artic.* I:231–265.

Swindale, M. V. 1981. Dendritic spines only connect. *Trends Neurosci.* 4:240–241.

Traub, R. D., and R. Llinas. 1979. Hippocampal pyramidal cells: significance of dendritic ionic conductances for neuronal function and epileptogenesis. *J. Neurophysiol. (Bethesda).* 42:476–496.

Turner, D. A. 1982. Soma and dendritic spine transients in intracellularly-stained hippocampal neurons. *Neurosci. Abstr.* 8:945.

Turner, D. A. 1983. Dendritic spine EPSPs in CA1 pyramidal cells—active or passive transfer from spine to soma? *Neurosci. Abstr.* 9:734.

Turner, D. A. 1984. Segmental cable evaluation of somatic transients in hippocampal neurons (CA1, CA3, and dentate). *Biophys. J.* 46:73–84.

Turner, D. A., and P. A. Schwartzkroin. 1980. Steady-state electrotonic

analysis of intracellularly-stained hippocampal neurons. *J. Neurophysiol. (Bethesda)*. 44:184–199.

Turner, D. A., and P. A. Schwartzkroin. 1983. Electrical characteristics of dendrites and dendritic spines in intracellularly-stained CA3 and dentate hippocampal neurons. *J. Neurosci.* 3:2381–2394.

Wenzel, J., W. Kirsche, G. Kune, T. Neumann, H. Wenzel, and E. Winkelman. 1973. Licht- und electronen Mikroskopische Untersuchungen uber die dendriten Spines an Pyramiden-Neuronen des Hippocampus (CA1) bei der Ratte. *J. Hirnforsch.* 13:387–408.

Wenzel, J., C. Stender, and G. Duwe. 1981. The development of the neuronal structure of the fascia dentata of the rat. Neurohistologic, morphometric, ultrastructural and experimental investigations. *J. Hirnforsch.* 22:629–683.

Westrum, L. E., and T. W. Blackstad. 1962. An electron microscopic study of the stratum radiatum of the rat hippocampus (CA1) with particular emphasis on synaptology. *J. Comp. Neurol.* 119:281–309.

Wong, R. K. S., D. A. Prince, and A. I. Basbaum. 1979. Intradendritic recordings from hippocampal neurons. *Proc. Natl. Acad. Sci. USA.* 76:986–990.